DOI: 10.37190/ ABB-02397-2024-04

Impact of Lower Limb Movements on Iliac Vein Stenting in Iliac Vein Compression Syndrome Patients: Insights from Computational Modeling

Jian Lu[1], Zhenmin Fan[1]*, Xia Ye[1], Xiaoyan Deng[2], Hai Feng*[3], Mingyuan Liu*[3]

[1]School of Mechanical Engineering, Jiangsu University of Technology, China
[2]Key Laboratory for Biomechanics and Mechanobiology of Ministry of Education, School of Biological Science and Medical Engineering, Beihang University, China;
[3] Department of Vascular Surgery, Beijing Friendship Hospital, Capital Medical University; Beijing Center of Vascular Surger, China
*Corresponding author: Zhenmin Fan, School of Mechanical Engineering, Jiangsu University of Technology, China, e-mail address: fanzhenmin2009@163.com;
Hai Feng, Department of Vascular Surgery, Beijing Friendship Hospital, Capital Medical University; Beijing Center of Vascular Surger, China, e-mail address: dr.mingyuanliu@pku.edu.cn;
Mingyuan Liu, Department of Vascular Surgery, Beijing Friendship Hospital, Capital Medical University; Beijing Center of Vascular Surger, China, e-mail address: vascusugfh@ccmu.edu.cn

Submitted: 6th February 2024
Accepted: 15th April 2024

Key Findings: Computational modeling demonstrated that hip and ankle movements significantly impact blood flow within the post-stented iliac vein. Active ankle exercise and intermittent pump compression lead to a significant reduction of the risk of thrombosis.

Take home Message: Post-stenting patients undergoing hip and ankle movements exhibit significant changes in blood flow within the treated iliac vein. Active ankle exercise and intermittent pump compression notably improve the hemodynamic environment.

Abstract:

Objective

Iliac vein stenting is the primary treatment for patients with iliac vein compression syndrome (IVCS). However, post-stent placement, patients often experience in-stent restenosis and thrombosis. Despite this, the role of lower limb movements in the functioning of stents and veins in IVCS patients remains unclear. This study aimed to address this knowledge gap by developing a computational model using medical imaging techniques to simulate IVCS after stent placement.

Methods

This research used a patient-specific model to analyze the effects of lower extremity exercises on hemodynamics post-stent placement. We conducted a comprehensive analysis to evaluate the impact of specific lower limb movements, including hip flexion, ankle movement, and pneumatic compression, on the hemodynamic characteristics within the treated vein. The analysis assessed parameters such as wall shear stress (WSS), oscillatory shear index (OSI), and residence time (RRT).

Results

The results demonstrated that hip flexion significantly disrupts blood flow dynamics at the iliac vein bifurcation after stenting. Bilateral and left hip flexion were associated with pronounced regions of low WSS and high OSI at the iliac-vena junction and the stent segment. Additionally, active ankle exercise (AAE) and intermittent pump compression (IPC) therapy were found to enhance the occurrence of low WSS regions along the venous wall, potentially reducing the risk of thrombosis post-stent placement. Consequently, both active joint movements (hip and ankle) and passive movements have the potential to influence the local blood flow environment within the iliac vein after stenting.

Conclusion

The exploration of the impact of lower limb movements on hemodynamics provides valuable insights for mitigating adverse effects associated with lower limb movements post iliac-stenting. Bilateral and left hip flexions negatively impacted blood flow, increasing thrombosis risk. However, active ankle exercise and intermittent pump compression therapies effectively improve the patency.

Key words: iliac vein compression syndrome, hemodynamics, iliac vein stenting, lower limb movement

1 Introduction

Iliac vein compression syndrome (IVCS), also known as May-Thurner syndrome or Cockett syndrome, is characterized by lower limb pain, swelling, venous stasis ulcers, and skin discoloration. These symptoms arise from the compression of the iliac vein by the overlying iliac artery and adjacent sacrum [4]. The prevalence of IVCS ranges from 20-34%[14], with a higher occurrence among young women aged 20-40 years, and a ratio of approximately 8:1 between left and right veins[30]. To date, iliac vein stenting has emerged as a preferred approach for managing thrombotic or non-thrombotic iliac vein lesions [7, 21, 23, 29]. Nevertheless, postoperative complications have consistently plagued patients. In-stent restenosis (ISR) has often occurred iliofemoral venous stents but has not been well described. It has

been reported to develop in >70% of patients who have undergone iliofemoral venous stenting[33]. In particular, post-stenting thrombosis in iliofemoral venous stents is a recurrent challenge, with reports suggesting thrombosis occurrence in over 70% of patients post-stenting [27, 40]. This high incidence of ISR underscores the need for further research and intervention strategies. Given these challenges, there is an imperative demand to refine and improve the clinical outcomes associated with iliac vein stenting.

Post-stenting thrombosis is intricately linked to deviant hemodynamic properties. Elevated blood flow velocities proximal to the stent strut have been observed to induce intermediate cells to release copious amounts of von Willebrand factor (vWF), which in turn promotes platelet activation and their subsequent adherence to collagen fibers [22]. In contrast, regions adjacent to struts exhibiting low or oscillatory wall shear stress (WSS) are conducive to the adhesion and aggregation of activated platelets, predisposing to thrombotic manifestations [9]. Empirical studies have elucidated that protruding stents are concomitant with detrimental hemodynamic features. Moreover, an increased stent thickness impedes the laminar flow within the vessel, instigating flow separation and recirculation [8, 9, 22, 38], thereby augmenting the propensity for stent thrombosis. Non-streamlined stent struts not only perturb the flow dynamics more pronouncedly but also augment the extent of flow separation [24]. Improper stent placement can further amplify the disturbance in blood flow dynamics, and misalignment or overlapping of stent struts can establish a pronounced reflux zone, heightening the risk of unfavorable clinical outcomes [10]. Thus, aberrant hemodynamic parameters emerge as pivotal factors influencing the success of IVCS stenting.

The dynamic environment of blood flow hemodynamics post-IVCS stenting is significantly influenced by movements of the lower limbs and the hip. Physiologically, the geometry of the iliofemoral vein is significantly modulated by hip movements[3]. An investigation encompassing 21 subjects post-iliac vein stenting delved into the effects of various hip joint rotation angles [3]. The data elucidated that among the movements, hip flexion predominantly affected parameters such as the curvature radius, stent axial length, and the femoral vein's minimum minor diameter. In parallel, the femoropopliteal artery undergoes distinct deformations, ranging from axial compression to bending, contingent on body postures like standing (180 degrees), sitting (90 degrees), and walking (110 degrees) [25]. Such geometric alterations, induced by diverse physical activities, can modulate the venous blood flow dynamics, thereby potentially altering the vein's physiological function. Wood et al. identified a pronounced association between post-lower limb movement blood flow patterns and vessel curvature[39]. Preliminary insights suggested that prolonged leg bending could compromise the endothelial function within the popliteal artery, manifesting as a marked decrement in blood flow and an expansion of regions with low WSS. Sedentary behavior, exemplified by uninterrupted sitting for 6 hours, was observed to substantially attenuate blood flow velocity and shear rate in both the popliteal and brachial arteries[28]. Complementing this, research indicated that post-stenting lower limb exercises precipitated the emergence of extensive low WSS zones within the femoral popliteal artery stent region [5, 6].

Certain lower limb activities can enhance lower limb blood flow. Active ankle exercise (AAE), also termed ankle pump movement, is a simple yet effective technique that fosters positive hemodynamic properties [12]. Similarly, in vitro medical tools like intermittent pneumatic compression (IPC) devices also promote beneficial hemodynamics [15]. Thus, both active and passive lower limb exercises significantly influence the hemodynamic state post-iliac vein stenting. These activities can either amplify or optimize blood circulation, impacting stent intervention outcomes. However, in-depth studies elucidating these clinical dynamics are scant. This research crafted a postoperative human iliac vein stent model and utilized numerical simulations to assess the effects of diverse lower limb movements, such as

hip and ankle actions, on postoperative blood flow metrics like time-averaged wall shear stress (TAWSS), oscillating shear stress index (OSI), and relative residence time (RRT). The study also delved into the ramifications of induced exercise and its combined effects on stent segment blood flow.

2 Method

The flowchart is depicted in Figure 1.

2.1 The computational models after stenting

This study received approval from the Ethics Committee of Beijing Friendship Hospital (Beijing, China) and adhered to the principles outlined in the Declaration of Helsinki. Additionally, the study protocol was submitted to the Medical Ethics Committee of this hospital. All participants in the study were provided with comprehensive information about the study and provided their informed consent by signing the appropriate documentation.

The acquisition of Computed tomography angiography (CTA) images for a 61-year-old female, spanning from the femoral vein to the inferior vena cava, was performed using an imager as depicted in Figure 1 (step 1, a). A total of 518 slices were obtained, with each section having a thickness of 1mm and an in-plane pixel size of 0.683mm. The lumen outline of iliac vein bifurcations was manually segmented from Minics19.0 (Materialise corporation, Belgium). Subsequently, the iliofemoral vein was reconstructed and the center line was extracted. The original model was then smoothed using Geomagic12.0 (Geomagic studio, USA) (see Figure 1, step 2). The final overall model length (L_0) is 480mm, the length from IVC to FV (L_1) is 170mm, and the length from the bending position to the FV (L_2) is 140mm (refer to Figure 2. 2(A)). The cross-section size of the maximum compression measures approximately 23×6.5mm.

In this study, the commercially available Wallstent（Boston Scientific Corp） was utilized for intervention. The stent strut exhibited a thickness of 0.25 mm, while its length measured 62 mm. The stent is emplaced into the inferior vena cava to prevent stent movement[20]. The outer diameter of the stent was approximately 1.1 to 1.2 times larger than the non-stenosis vein lumen[3, 26]. In Figure 1, Step 2, the 3D modeling software Solidworks 2020 (Solid Works Corp, Concord, MA) was employed to substitute the compression zone and integrate it along the central axis of the lumen.

To examine the impact of hip movements on the host vein subsequent to IVCS stenting, the vein in the supine position was flexed to simulate the hip motion. As depicted in Figure 2(B), the point of flexion of the vein is situated 2-3 cm upstream from the highest point of the iliac crest, with a bending angle of 75° and a bending radius of 67.5mm[3, 36]. There exist four distinct categories of hip joint movements, namely: body straight (supine), hip joint flexion in both legs (sitting), and unilateral hip joint flexion caused by left and right legs.

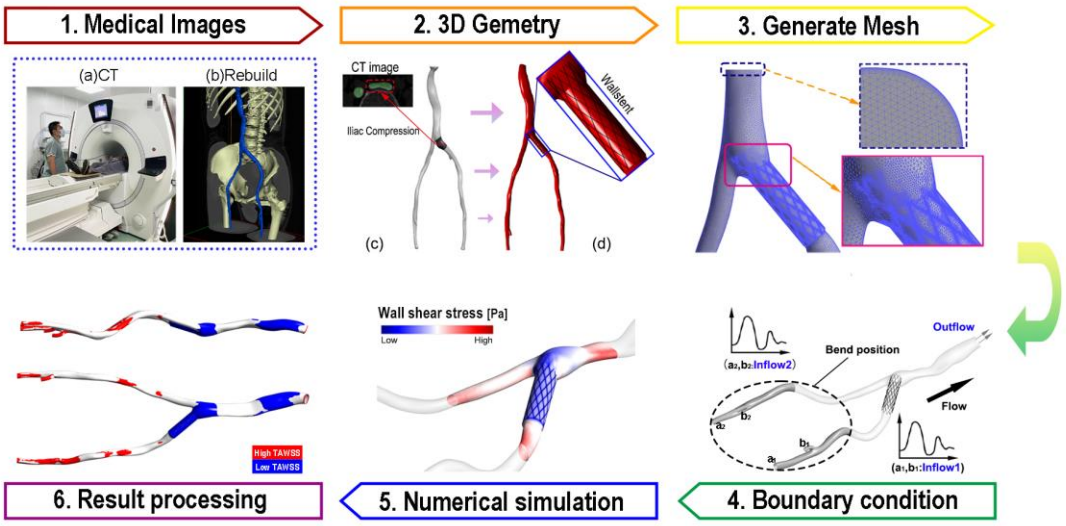

Figure 1 The methodology employed in this study. In Step 1, the computed tomography slices were acquired using a CT scanner, and subsequently, the model was reconstructed. Step 2 involved the smoothing of the original model and the subsequent implantation of the iliac vein stent. Step 3 encompassed the generation of a computational mesh, which included a boundary layer and local refinement. In Step 4, the appropriate boundary conditions were applied to the computational models. Step 5 involved the execution of a computational fluid dynamics (CFD) simulation. Finally, in Step 6, the results were analyzed and subjected to post-processing.

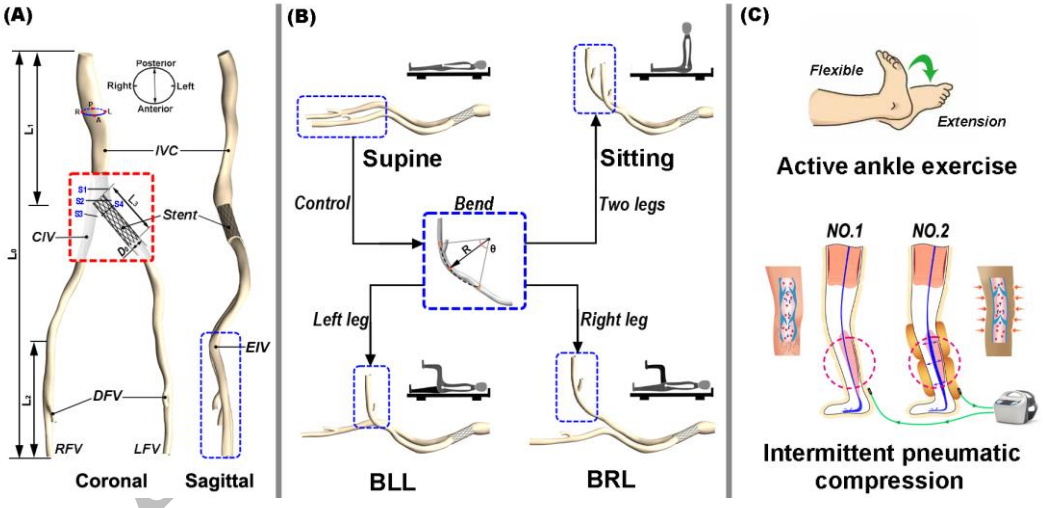

Figure 2 Geometric models of the iliofemoral vein with a stent after various lower limb movements. ((A) Iliofemoral vein model includes deep femoral vein (DFV), left femoral vein (LFV), right femoral vein (RFV), external iliac vein (EIV), common iliac vein (CIV) and inferior vena cava (IVC). (B) The models respectively are body straight (supine), hip joint flexion in both legs (sitting), and unilateral hip joint flexion caused by left (Bend left leg, BLL) and right (Bend right leg, BRL) legs. (C) Active ankle exercise (AAE) and intermittent pneumatic compression (IPC) therapy in the sitting position.

2.2 Governing Equation

In our analysis, we make the assumption that the blood flow within the lumen is characterized by laminar homogeneity, incompressibility[19], and is governed by the incompressible liquid Navier-Stokes

equation[1, 34].

$$\rho\left(\frac{\partial u}{\partial t} + u \cdot \nabla u\right) = -\nabla p + \nabla \cdot \tau, \quad (1)$$

$$\nabla \cdot u = 0\ , \quad (2)$$

where **u** and p are the three-dimensional velocity vector field and pressure field in the iliac vein, and ρ represents the density (ρ=1060 kg/m^3) of blood flow [19]. The blood flow has the typical non-Newtonian behavior, which is described as the Carreau-Yasuda model [17].

$$\tau = 2\mu(\dot{\gamma})S\ , \quad (3)$$

$$\eta(\dot{\gamma}) = \eta_\infty + (\eta_0 - \eta_\infty)[1 + (\lambda\dot{\gamma})^2]^{\frac{n-1}{2}}\ , \quad (4)$$

where S and standard $\dot{\gamma}$ are the rate of deformation tensor and shear rate, respectively. η_∞ and η_0 is the viscosity at infinite shear rate (η_∞=0.00345 kg/ms) and zero shear rate (η_0=0.056 kg/ms), λ represents the time constant (λ =3.31 s), and n represents the power law exponent (n=0.36).

2.3 Boundary conditions

Figure 3 displays the variations in inlet flow velocity (femoral vein) during different lower limb movements [31, 32]. In order to examine the impact of hip flexion, we examined the blood flow in four different states (as shown in Figure 3): the supine model, which simulates a supine position with both hips extended; the sitting model, which simulates a seated position with both hips flexed; the BLL model, which simulates left leg bending (left hip flexion); and the BRL model, which simulates right leg bending (right hip flexion). Additionally, to compare the effects of active and passive movement on the blood flow environment after stenting, we analyzed the femoral vein flow velocity under AAE, IPC. Figure (C) provides a schematic illustration of ankle joint movement and compression treatment, and AAE+IPC, and the inlet flow velocity waveforms were shown in Figure 3 (b). Outflow condition was adopted to at IVC. The venous wall and stent were treated as rigid wall with no slip.

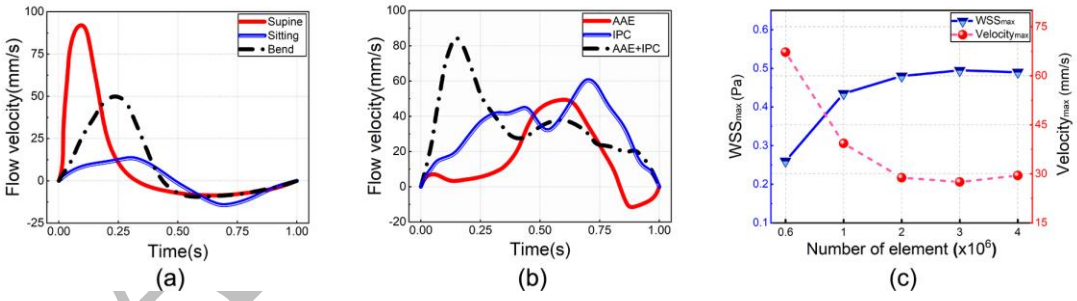

Figure 3 Flow velocity waveforms of iliofemoral vein after stenting under different movements and mesh independence analysis. ((a) Femoral vein flow velocity waveforms under different hip movements. (b) Femoral vein flow velocity waveform under ankle exercise and IPC treatment. (c) Changes in WSS max and Velocity max when the number of grid numbers included 0.6,1,2,3, and 4 million)

2.4 Calculation process

All models employed in this paper utilize ICEM CFD (ANSYS, Inc, Canonsburg, the United States) to generate tetrahedral and hexahedral elements, incorporating 10 boundary layers. The initial layer possesses a height of 0.02mm and a growth rate of 1.2 to fulfill the prerequisites of laminar flow simulation. To precisely capture the blood flow characteristics in the vicinity of the stent, local refinement was performed at this specific location (Figure 1, step 3). The density of the mesh plays a crucial role in

determining the accuracy of the calculations. Consequently, this study establishes five models, progressively increasing the number of mesh cells from 0.64 to 4.8 million. Ultimately, it has been determined that the relative error of two cases is less than 5% when the number of grids exceeds 2 million, thereby substantiating the independence of the grids. To optimize computational expenses, the maximum element size for this model has been established as 1.5 mm, resulting in approximately 3.4 million cells.

The numerical simulation employed Fluent 20.0 (ANSYS, Inc, Canonsburg, the United States), with a time step of 0.005s, 20 iterations per time step, and a convergence criterion of 1×10^{-5} for residual error. To ensure precise data analysis, the simulation utilized the second-order upwind Simple algorithm. All data utilized for post-processing originates from the third cardiac cycle.

2.5 Hemodynamic analysis

To effectively depict the spatial distribution of wall shear stress (WSS) within a singular cardiac cycle, this research employs the calculation of time-averaged WSS (TAWSS) for data analysis. The TAWSS is determined by the following equation[18]:

$$\mathrm{TAWSS} = \frac{1}{\mathrm{T}}\int_0^{\mathrm{T}} |\mathrm{WSS(s,t)}|\cdot \mathrm{dt}, \tag{5}$$

where t denotes the time, T represents the duration of the pulsation cycle, s signifies the position on the venous wall, and WSS denotes the wall shear stress vector at time t.

Additionally, the oscillatory shear index (OSI) is employed to assess alterations in WSS direction and fluctuations in velocity throughout the cardiac cycle, and it is defined as[18]:

$$\mathrm{OSI} = \frac{1}{2}\left[1 - \left(\frac{\left|\int_0^{\mathrm{T}} \mathrm{WSS(s,t)}\cdot \mathrm{dt}\right|}{\int_0^{\mathrm{T}} |\mathrm{WSS(s,t)}|\mathrm{dt}}\right)\right], \tag{6}$$

The relative residence time (RRT) is introduced as a parameter to quantify the relative duration of blood flow, and its calculation is as follows[18]:

$$\mathrm{RRT} = \frac{1}{(1-2\cdot \mathrm{OSI}).\mathrm{TAWSS}}, \tag{7}$$

Furthermore, the areas with low TAWSS, high OSI, and high RRT were also incorporated to enable quantitative comparison of the hemodynamic parameters across the models. In this paper, these areas were denoted as LMSA, HOSA, and HRRA respectively. These "abnormal" areas are prone to causing lesions[13].

To more accurately capture the turbulent movement of blood within the lumen, we designate the flow in the direction opposite to the blood flow as reflux and quantify it using the reflux rate. This is expressed by

$$\text{Reflux rate} = \frac{F_w}{F_0}(\%), \tag{8}$$

where, F_w represents the volume of the specific region generating reflux flow and F_0 represents the volume of the entire fluid domain.

3 Results

3.1 Influence of hip movement on the treated iliac vein

Figure 4 presents the instantaneous streamline, color-coded by velocity magnitude, highlighting the profound impact of different movements on host vein streamlines. Specifically, the Sitting, BLL, and BRL models in Figure 4(a) show significant flow disturbances at locations I (above the iliac-vena junction) and II (iliac-vena junction). Among them, the BLL and BRL models, with hip flexion, manifest a pronounced vortex flow and low-velocity region at location II compared to the supine model, with BLL being the most affected. This disturbed flow in the BLL model even extends to the IVC junction. In

contrast, the Sitting model's streamlines in the bifurcated vessels align closely with the vessel wall. Both the Supine and BLL models show flow separation and recirculation at model III (proximal of right CIV), with the Supine model displaying notably reduced flow velocity and streamline density. Different motion states also influence stent segment flow. While the Sitting model shows consistent flow patterns at the stent segment, the BLL, Supine, and BRL models exhibit flow irregularities due to velocity disparities, with the BRL model showing the most significant disturbances.

To elucidate the velocity variations induced by hip movement, slices (S1, S2, S3, and S4) were chosen from four distinct regions. Notably, the Supine and Sitting models exhibited enhanced blood flow in the S1 section compared to the BRL and BLL models. The Supine model displayed a pronounced crescent-shaped high-velocity region on one side of the lumen, whereas the Sitting model had a uniform velocity. In contrast, the BRL and BLL models revealed a diminished flow velocity near the stent junction, with the BLL model being especially pronounced. Observations from the S2 slice, positioned at the junction, indicated significant flow disturbances around the stent as it enters the IVC. The Supine model manifested elevated velocities at the stent struts, while the Sitting and BLL models demonstrated increased velocities, with BLL recording the lowest. The velocity distribution in the S3 section, situated to the right of the proximal CIV, was analogous for the Supine and BLL models, with a high-velocity zone predominantly on one side of the right CIV. In contrast, the Sitting and BRL models yielded elevated velocities throughout the lumen. Additionally, hip movements influenced the flow characteristics on the S4 slice, located at the stent's proximal end. The Supine and BRL models displayed an eccentric "crescent shape" high-velocity pattern near the wall, with reduced velocities at the lumen's corner. The flow velocities between the Sitting and BLL models were relatively consistent, but their flow directions on this slice were markedly divergent.

To quantitatively assess the impact of varied hip movements on the host iliac vein's blood flow, we computed the reflux flow rate at both the iliac junction and the entire stent segment, as depicted in Figure 4 (c-1) and (c-2). The figure reveals that the junction's reflux rate significantly exceeded that of the stent segment. Notably, the BLL model exhibited the highest reflux at the junction, whereas the Sitting model had the lowest. Furthermore, within the stent segment, the BLL model had the highest reflux rate. The reflux rates of the Supine and BLL models were nearly identical, approximately twice that of the BRL model.

The influence of diverse hip movements on the distribution of TAWSS, OSI, and RRT following iliac vein stenting were demonstrated on Figure 5. As illustrated in Figure 5(a), all models manifested reduced WSS at the stent strut, with the Sitting and BLL models also presenting a pronounced low WSS region at the venous wall spanning the entire stent segment. The Sitting model exhibited the most extensive LMSA, succeeded by the BLL model, with their low WSS regions markedly surpassing other models. High WSS was discernible in the right CIV of both the Supine and BLL models and intermittently at the stent segment's extremities in the BRL models. Figure 5(b) highlights areas of elevated OSI primarily at the iliac vein and vena cava junction and at the stent segment's ends, with the most expansive high OSI regions observed in the Sitting and Supine models. The distribution of high RRT regions, as portrayed in Figure 5(c), mirrored that of low WSS areas, predominantly located at the iliac-vena junctions and stent segments. The Sitting and BLL models displayed a significant high RRT region within the stent segment, while the BRL model showcased it at the junction. Notably, the Sitting model had the most expansive HRRA on the venous wall, followed by BLL, both considerably exceeding the Supine and BRL models. Subsequent statistical evaluations indicated a more than 35-fold surge in LMSA for the Sitting and BLL models relative to others, with the stent segment constituting over 78.5%

of the aggregate area in the primary model. The BLL model exhibited the most pronounced HOSA, 2.5 times that of the Sitting model. The HRRA in the Supine and BLL models was over 3.3 times that of other models, with the stent segment representing roughly 64.3% of the total area. Thus, hip movement markedly amplified the LMSA and HRRA regions post-intervention.

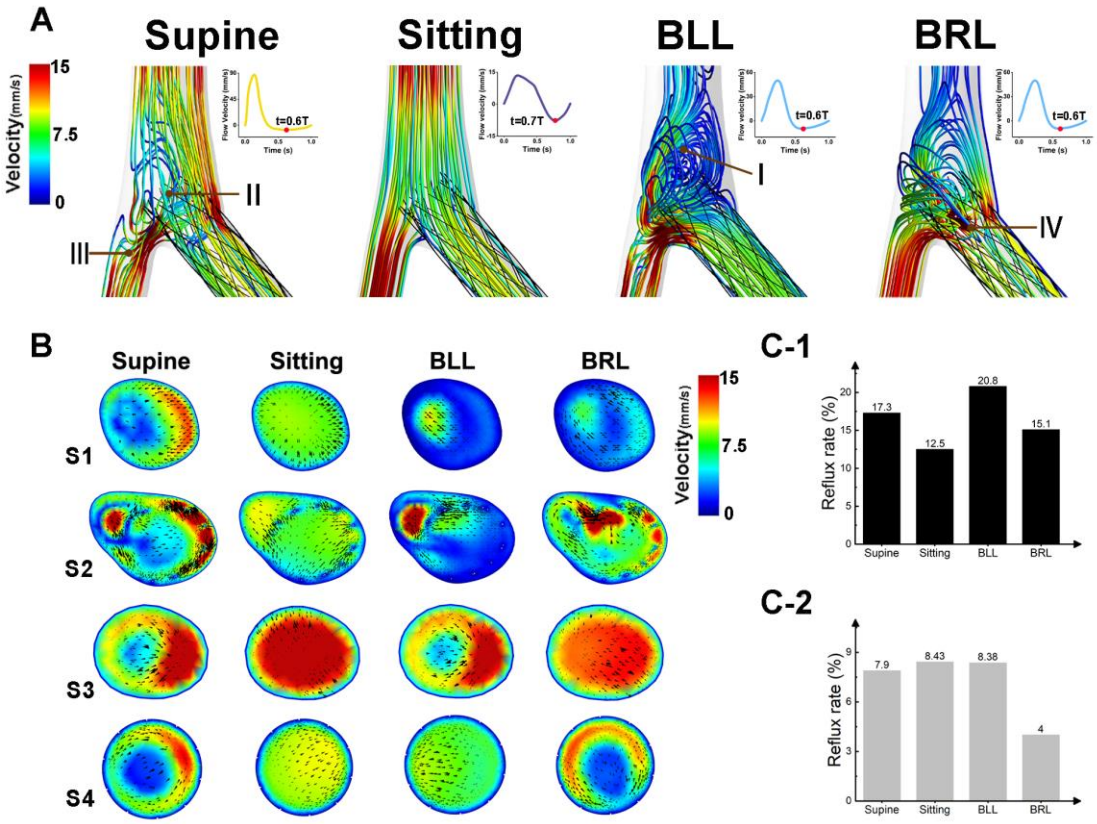

Figure 4 Effect of hip movement on blood flow of the treated iliac vein (The models respectively are body straight (Supine), hip joint flexion in both legs (Sitting), and unilateral hip joint flexion caused by left (Bend left leg, BLL) and right (Bend right leg, BRL) legs.). (a)The streamline of each model at the peak diastolic moment. (b) Contours of the axial velocity and the velocity vectors at S1, S2, S3 and S4 locations of the venous slices. (c-1) Reflux flow rate of all models in the junction. (c-2) Reflux flow rate of all models in the stent. (Regions I, II, III, IV were located the downstream of iliac-vena junction, iliac-vena junction, the proximal of right CIV and the proximal of stent, respectively.)

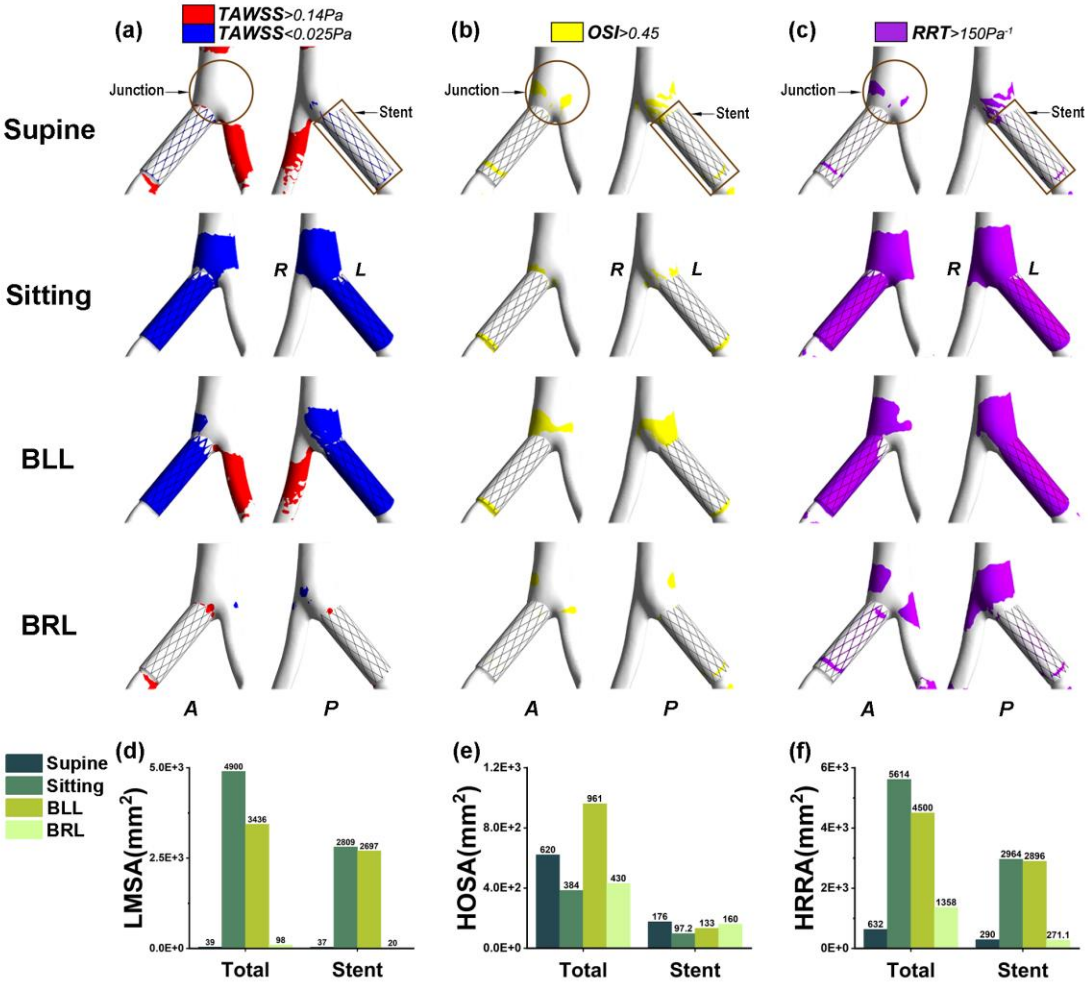

Figure 5 (a), (b) and (c) are the distribution clouds of TAWSS, OSI, and RRT in iliac vein models under different hip movements. (d), (e) and (f) are the areas occupied by TAWSS<0.025Pa, OSI>0.45, and RRT>150 Pa-1 in the venous wall and stent segments, respectively. (The models respectively are body straight (Supine), hip joint flexion in both legs (Sitting), and unilateral hip joint flexion caused by left (Bend left leg, BLL) and right (Bend right leg, BRL) legs.)

3.2 Effects of ankle movement and external treatment on the treated iliac vein

Figure 6 illustrates the observed flow pattern in the iliac vein, with particular emphasis on the influence of AAE and external treatment on blood flow. When compared to the resting state, all lower limb exercises led to heightened velocity within the lumen during diastole. It is worth noting that the single AAE model displayed disrupted flow in the region of I (iliac-vena junction) with a slight increase in blood flow, whereas the models receiving IPC treatment exhibited significantly increased blood flow in most areas of the iliac vein.

To demonstrate the distribution of blood flow in the iliac vein post-stenting, representative slices (S1, S2, S3 and S4) were examined. It was also evident that both AAE and IPC interventions exhibited a certain degree of improvement in the axial velocity of blood flow, while the AAE alone model did not exhibit a significant increase. Figure 6(b) illustrates that the blood flow in the Resting and AAE models remained relatively uniform on S1 slice, whereas the application of IPC induced an eccentric high-speed region on one side of the lumen. The Resting and AAE models demonstrated a significant concentration

of disturbed flow in close proximity to the stent struts on S2 section, whereas the other two models did not exhibit evident disturbed flow and instead display a "high-low-high" distribution pattern from the external to internal of lumen. On the S3 slice, the flow velocity distribution of the Resting and IPC treated models was characterized by high velocity in the core and low velocity near the venous wall. Conversely, the AAE model exhibited a high velocity distribution near the wall on this slice. In comparison to the Resting and AAE models, the models receiving IPC demonstrated a significant increase in blood flow on slice S4. Notably, the models treated with both AAE and IPC exhibited the highest elevation in blood flow.

According to the histogram of the reflux flow rate at the iliac-vena junction and entire stent segment which is shown in the Figure 6(c-1) and (c-2), we can see that, the reflux rate at the junction was much higher than that at the stent segment. The paper also found the degree of the reflux flow of the AAE model at the junction was the maximum, while that of the Resting was the second, and the IPC model has the minimum reflux rate of all models. Additionally, the reflux rate of the four models was gradually decreasing from Resting to AAE+IPC model, and we easily found that the reflux rate of Resting models at the stent regions was over 1.5 times than that of the AAE+IPC model.

Figure 7 assesses the impact of AAE and IPC interventions on the wall TAWSS, OSI, and RRT of the treated vein. Figure 7 (a) illustrates that all models display varying degrees of low WSS regions near the stent struts. The Resting model exhibited a low WSS region that extended throughout the venous wall of the entire stent segment and the iliac-vena junction. In contrast, the AAE model only had a small amount of low WSS near the stent struts and the junction, and these regions almost disappeared after receiving IPC. The Resting model had the largest LMSA on the venous wall, followed by the AAE model. The low WSS regions in these two models surpassed that of the receiving IPC models. However, in the two IPC models, a substantial expanse of regions with high WSS emerged upstream of CIV and stent segment. Figure 7 (b) illustrates that the regions with high OSI in the three models after different treatments are noticeably less dispersed at both ends of the stent segment compared to the Resting model, although the disparity between them was not statistically significant. Furthermore, the Resting model exhibited a greater distribution of regions with high OSI at the junction of the iliac vein and the overall venous wall of the stent segment. The distribution of the area with high RRT in Figure 7 (c) mirrored the distribution of low WSS. High RRT was primarily concentrated at the junction and stent segments, particularly in the Sitting and AAE models where the HRRA was significantly larger compared to other models. In terms of the venous wall, the Resting model exhibits the highest HHRA, followed by the AAE model, which surpassed the two IPC models by a significant margin. The histogram presented in Figure 7(d)-(f) further examines the extent of adverse blood flow in the vein after stenting. In both the Resting and AAE models, the LMSA was approximately 19.5 and 6.5 times greater, respectively, than that of the two IPC models, with the stent segment accounting for over 52% of this area. However, the localization of the LMSA in the two IPC models was predominantly observed at the stent segment, accounting for more than 84%. Comparatively, the Resting model exhibited the largest HOSA, surpassing the other models by more than 11 times, while the HOSA of the three lower limb movement models displayed minimal variation (Figure 7(e)). Additionally, in Figure 7(f), the HRRA in the Resting and AAE models was more than 3.8 times larger than that of the other models, with the stent segment occupying approximately 41.5% of this area. Consequently, the implementation of AAE and IPC treatment significantly enhanced the LMSA, HOAS, and HRRA.

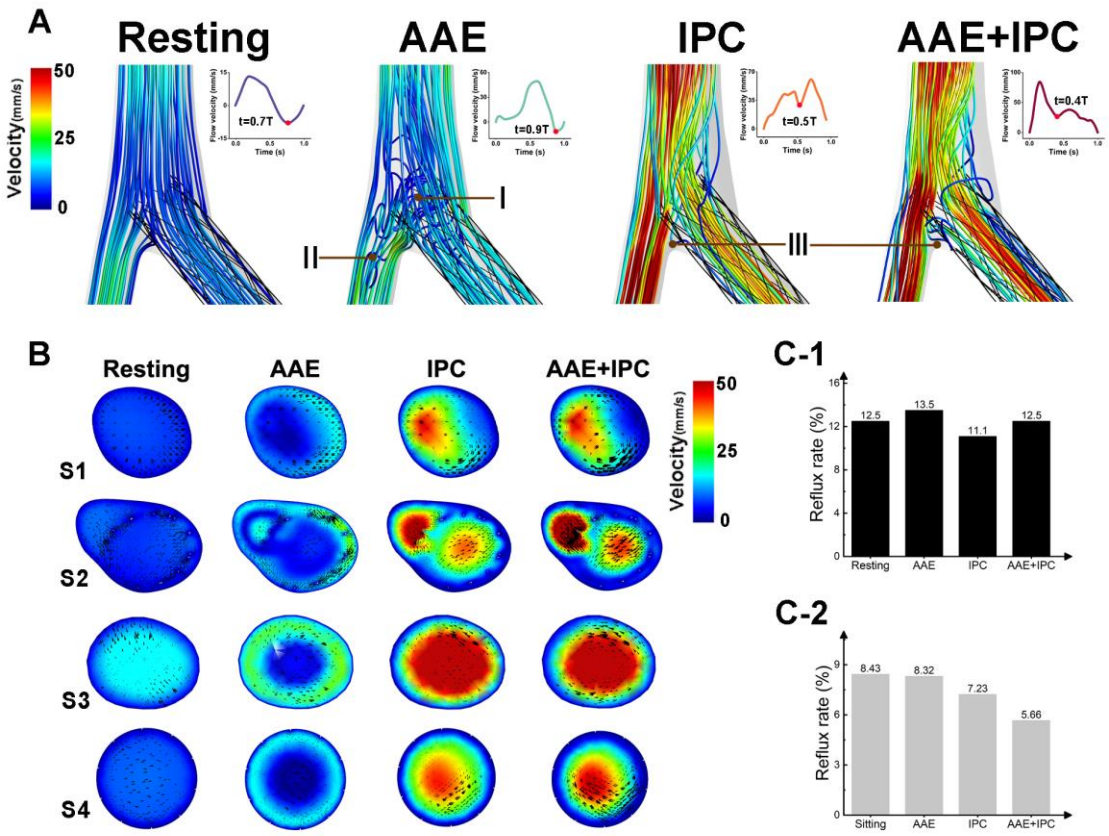

Figure 6 Effect of ankle movement and intermittent pneumatic compression on blood flow after iliac vein stenting. (a) Streamlines of the treated iliac vein models at the peak diastolic moment. (b) Contours of the axial velocity at location of the slice S1, S2, S3 and S4. (c-1) Reflux flow rate of all models in the junction. (c-2) Reflux flow rate of all models in the stent. (Regions I, II and III are iliac-vena junction, right proximal CIV and inferior junction, respectively.) (The models respectively are human body after rest (Resting), active ankle exercise (AAE), intermittent pneumatic compression (IPC), and AAE combined IPC (AAE+IPC) therapy in the sitting position)

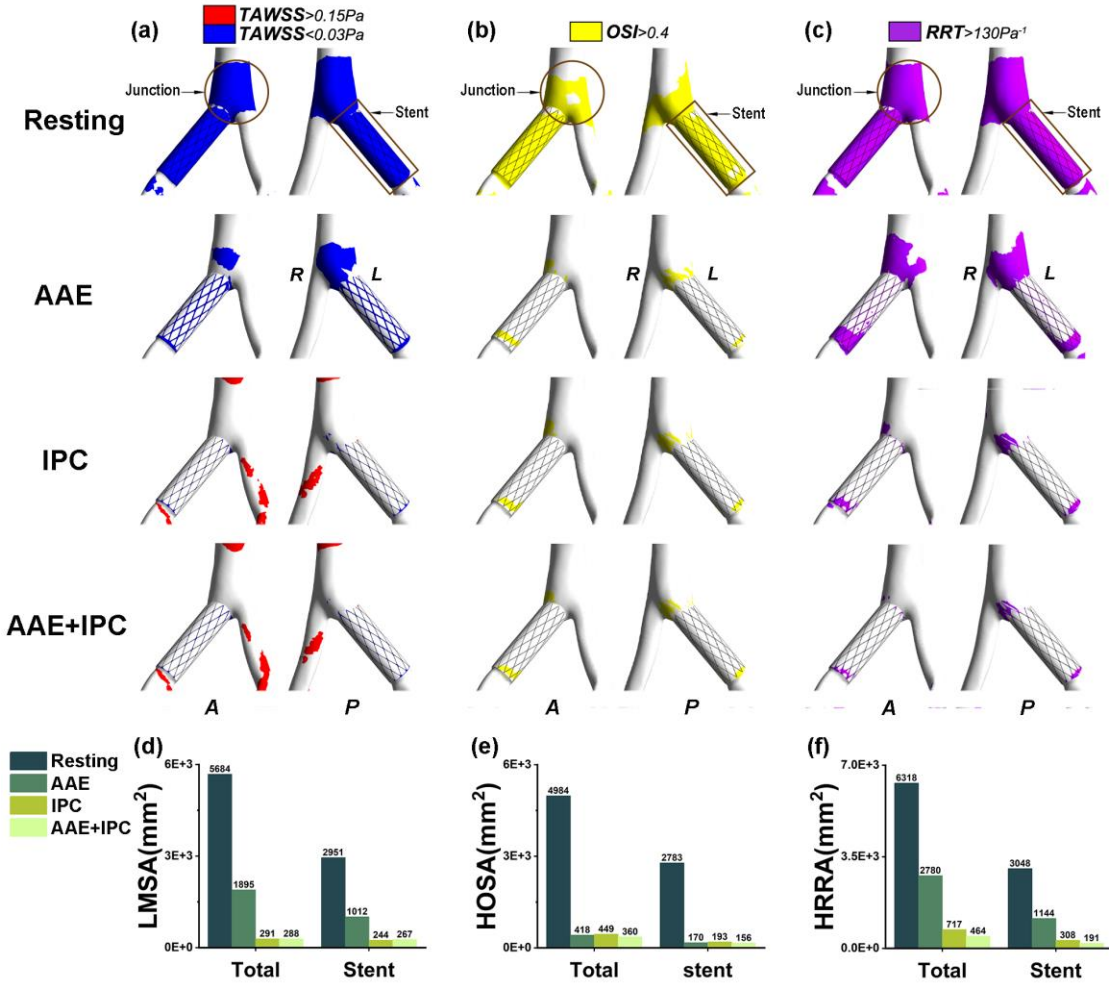

Figure 7 (a), (b) and (c) show the distribution of TAWSS, OSI, and RRT in ankle exercise and intermittent pneumatic compression, respectively. (d), (e) and (f) are the areas of TAWSS<0.03Pa, OSI>0.4, RRT>130Pa-1 in the whole model and stent segment, respectively. (The models respectively are human body after rest (Resting), active ankle exercise (AAE), intermittent pneumatic compression (IPC), and AAE combined IPC (AAE+IPC) therapy in the sitting position)

4 Discussion

Iliac venous stenting, a common treatment for IVCS, often faces complications like postoperative thrombosis and in-stent restenosis, leading to suboptimal postoperative outcomes[27, 40]. This research delves into the biomechanical conditions post-venous stenting, factoring in the effects of various lower limb movements, to elucidate the mechanisms behind these complications. It also evaluates how active limb movement and external treatments influence the hemodynamic environment within the host vein.

The induction of abnormal blood flow in the host vein was observed following stenting. The numerical simulation findings from this investigation revealed the presence of unfavorable local blood flow (such as reflux, flow separation, low WSS, high OSI and RRT, etc.) in the bifurcated vein, irrespective of the lower limb's motion states. These unfavorable conditions may contribute significantly to the unsatisfactory clinical outcomes observed after vein stenting [5, 6, 11]. This occurrence can potentially be attributed to the intricate spatial configuration of the bifurcated vein, which different from that of carotid arteries and coronary arteries. Clinical studies have yielded evidence indicating that sedentary and prolonged lying behaviors are correlated with an elevated susceptibility to peripheral artery disease

[35]. Continuous sitting hampers blood circulation and diminishes vascular endothelial function in the lower extremities, thereby fostering the development of thrombus in the legs[35]. Another observation found that extended legs also showed a gradual decrease in blood flow during prolonged lying, which may be related to persistent lower limb immobility, but this decrease in blood flow and shear rate was not sufficient to impair popliteal artery endothelial function during straight legs[37].

Nevertheless, certain exercises may exacerbate the generation of detrimental blood flow patterns. Our study discovered that the Supine and BRL positions exhibited smaller areas of low WSS and high RRT, whereas Sitting and BLL positions demonstrated the highest degree of disturbed flow. When the human body is in a supine position, extending the legs results in an increased blood flow of bilateral veins, thereby partially mitigating the disrupted flow. Conversely, when the hip is flexed, local blood flow is significantly impacted. The flexion of the left leg subsequent to intravascular ultrasound-guided iliac vein stenting results in chaotic blood flow near the bifurcation, accompanied by flow separation. This blood flow is particularly pronounced in the BLL model. These empirical observations indicate that the flexion of the left leg following intravascular ultrasound-guided iliac vein stenting engenders the most anomalous hemodynamic milieu. This peculiarity may be attributed to geometric factors, such as the diameters of the left and right iliac veins and their disparate angles in relation to the vena cava. According to reports, the act of bending one leg has been found to promote the development of lower limb diseases [37]. Prolonged periods of continuous single-leg bending, exceeding 3 hours, have been identified as a contributing factor to the occurrence of femoropopliteal atherosclerosis and other related ailments. Furthermore, clinical observations have revealed that crossing legs increases the susceptibility to chronic venous insufficiency (CVI) in the lower limbs, such as varicose veins (VV) [41]. This study highlights the impact of asymmetry in the left and right iliac veins, which exacerbates the blood flow environment at the bifurcation, thereby providing a significant theoretical foundation for understanding these clinical phenomena. Hence, this study does not advocate the prolonged flexion of a single leg, particularly the left leg, following stenting. Nonetheless, it is our contention that exercise is indeed beneficial, but it should be performed in an alternating manner to better mitigate the prolonged detrimental impact of blood flow on the venous wall. We believe that the implementation of alternating lower limb movements could potentially yield favorable outcomes in enhancing the blood flow environment subsequent to stent implantation. In addition to its capacity for mitigating muscle tension and fostering metabolic processes, lower limb exercise has the potential to ameliorate the enduring repercussions of an unfavorable blood flow environment on endothelial cells. Moreover, it can exert positive effects such as enhancing blood circulation and averting venous embolism in the lower limbs, thereby enhancing the clinical efficacy of the host vein following stent placement.

Furthermore, this study has revealed that both AAE and IPC interventions can effectively suppress the abnormal hemodynamic features in the host vein after intervention. The simulation results demonstrated that AAE exerted a significant inhibitory effect on adverse blood flow following stenting, as compared to the resting state. Additionally, IPC treatment led to a substantial increase in peak velocity within the femoral vein, reaching a minimum of fourfold. This notable enhancement in blood flow rate holds the potential to effectively mitigate the occurrence of venous thrombosis, a crucial factor contributing to the favorable clinical outcomes observed with these two interventions in practical medical settings. These finding align with clinical observations that both AAE and IPC may possess substantial therapeutic efficacy in the prevention of DVT within clinical settings [31]. Many clinical experiments have also demonstrated that the use of IPC devices can lead to an elevation in venous pressure and wall shear stress[2]. These mechanical forces have been observed to elicit a diverse range of biological

responses in endothelial cells, thereby facilitating functions such as fibrinolysis, vasodilation, and antithrombotic therapy[2, 16]. Consequently, this investigation suggests that AAE and IPC may represent a more advantageous approach for modulating the blood flow environment and mitigating the risk of thrombosis.

Limitations

This study exhibits certain limitations. Specifically, it solely examines the influence of individual movements, disregarding the fact that lower limb movement typically comprises a combination of multiple movements. Nevertheless, studying the impact of individual movements is advantageous. Additionally, the study does not account for the alteration in blood vessel diameter after intervention, various exercises, and follow up post-stenting CT scans, which could potentially affect the outcomes. However, the limited impact of these changes is evident due to the absence of significant alterations in venous area.

5. Conclusion

Bilateral and left hip flexions negatively impacted blood flow, increasing thrombosis risk. However, AAE and IPC therapies effectively improved these conditions, enhancing physical efficacy.

Acknowledgements

This work is supported by National Natural Science Research Foundation of China (No. 12372305, 12272153, 82000429, 11902126), Social Development Science and Technology Support Project of Changzhou (CE20235044), and startup foundation of Jiangsu University of Technology (No. KYY16028), Zhongwu young innovative talents projection from Jiangsu Institute of Technology. Capital's Funds for Health Improvement and Research (CFH 2022-4-20217), Beijing Nova Program (No.20230484308), Young Elite Scientists Sponsorship Program by CAST (2023QNRC001), Beijing Municipal Hospital Scientific Research Training Program (PX2021002), Youth Elite Program of Beijing Friendship Hospital (YYQCJH2022-9), Science and Technology Program of Beijing Tongzhou District (KJ2023CX012).

Declaration of Conflicting Interests

All authors declare no competing interests.

References

[1] Ai L, Vafai K, *A coupling model for macromolecule transport in a stenosed arterial wall*, Int. J. Heat Mass Transfer, 2006, 49(9-10), 1568-91. http://doi.org/10.1016/j.ijheatmasstransfer.2005.10.041.

[2] Chen A, Frangos S, Kilaru S, Sumpio B, *Intermittent pneumatic compression devices–physiological mechanisms of action*, Eur J Vasc EndocascN, 2001, 21(5), 383-92. http://doi.org/10.1053/ejvs.2001.1348.

[3] Cheng CP, Dua A, Suh G-Y, Shah RP, Black SA, *The biomechanical impact of hip movement on iliofemoral venous anatomy and stenting for deep venous thrombosis*, J Vasc urg-Venous L, 2020, 8(6), 953-60. http://doi.org/10.1016/j.jvsv.2020.01.022.

[4] Cockett F, Thomas ML, *The iliac compression syndrome*, Brit J Surg, 1965, 52(10), 816-21. http://doi.org/10.1002/bjs.1800521028.

[5] Ferrarini A, Finotello A, Salsano G, Auricchio F, Palombo D, Spinella G, et al., *Impact of leg bending in the patient-specific computational fluid dynamics of popliteal stenting*, Acta Mech Sin, 2021, 37, 279-91. http://doi.org/10.1007/s10409-021-01066-2.

[6] Gökgöl C, Ueki Y, Abler D, Diehm N, Engelberger RP, Otsuka T, et al., *Towards a better understanding of the posttreatment hemodynamic behaviors in femoropopliteal arteries through personalized computational models based on OCT images*, Sci Rep, 2021, 11(1), 16633.

http://doi.org/10.1038/s41598-021-96030-2.
[7] Jeon UB, Chung JW, Jae HJ, Kim H-C, Kim SJ, Ha J, et al., *May-Thurner syndrome complicated by acute iliofemoral vein thrombosis: helical CT venography for evaluation of long-term stent patency and changes in the iliac vein*, Am J Roentgenol, 2010, 195(3), 751-7. http://doi.org/10.2214/AJR.09.2793.
[8] Koskinas KC, Chatzizisis YS, Antoniadis AP, Giannoglou GD, *Role of endothelial shear stress in stent restenosis and thrombosis: pathophysiologic mechanisms and implications for clinical translation*, J Am Coll Cardiol, 2012, 59(15), 1337-49. http://doi.org/10.1016/j.jacc.2011.10.903.
[9] Ku DN, Giddens DP, Zarins CK, Glagov S, *Pulsatile flow and atherosclerosis in the human carotid bifurcation. Positive correlation between plaque location and low oscillating shear stress*, Arterioscler., Thromb. Vasc Biol, 1985, 5(3), 293-302. http://doi.org/10.1161/01.ATV.5.3.293.
[12] Lagache M, Coppel R, Finet G, Derimay F, Pettigrew RI, Ohayon J, et al., *Impact of malapposed and overlapping stents on hemodynamics: a 2D parametric computational fluid dynamics study*, Mathematics-Basel, 2021, 9(1), 795. http://doi.org/org/10.3390/math9080795.
[13] Li C, Feng H, Wang X, Wang Y, *The influencing mechanism of iliac vein stent implantation for hemodynamics at the bifurcation*, Comput Methods Biomech, 2022, 1-10. http://doi.org/10.1080/10255842.2022.2120352.
[14] Li T, Yang S, Hu F, Geng Q, Lu Q, Ding J, *Effects of ankle pump exercise frequency on venous hemodynamics of the lower limb*, Clin Hemorheol Microcirc, 2020, 76(1), 111-20. http://doi.org/10.3233/CH-200860.
[15] Li X, Liu X, Li X, Xu L, Chen X, Liang F, *Tortuosity of the superficial femoral artery and its influence on blood flow patterns and risk of atherosclerosis*, Biomech Model Mechanobiol, 2019, 18, 883-96. http://doi.org/10.1007/s10237-019-01118-4.
[16] Liu J, Liu P, Xia K, Chen L, Wu X, *Iliac vein compression syndrome (IVCS): an under-recognized risk factor for left-sided deep venous thrombosis (DVT) in old hip fracture patients*, Med Sci Monitor, 2017, 23, 2078. http://doi.org/10.12659/MSM.901639.
[17] Maffiodo D, De Nisco G, Gallo D, Audenino A, Morbiducci U, Ferraresi C, *A reduced-order model-based study on the effect of intermittent pneumatic compression of limbs on the cardiovascular system*, P I Mech Eng H, 2016, 230(4), 279-87. http://doi.org/10.1177/0954411916630337.
[18] Morbiducci U, Gallo D, Massai D, Consolo F, Ponzini R, Antiga L, et al., *Outflow conditions for image-based hemodynamic models of the carotid bifurcation: implications for indicators of abnormal flow*, J. Biomech Eng, 2010, 132(1), 1005-1015. http://doi.org/10.1115/1.4001886.
[19] Morbiducci U, Gallo D, Ponzini R, Massai D, Antiga L, Montevecchi FM, et al., *Quantitative analysis of bulk flow in image-based hemodynamic models of the carotid bifurcation: the influence of outflow conditions as test case*, Ann Biomed Eng, 2010, 38, 3688-705. http://doi.org/ 0.1007/s10439-010-0102-7.
[20] Murphy EH, Johns B, Varney E, Buck W, Jayaraj A, Raju S, *Deep venous thrombosis associated with caval extension of iliac stents*, J Vasc Surg-Venous L, 2017, 5(1), 8-17. http://doi.org/10.1016/j.jvsv.2016.09.002.
[21] Neglén P, Hollis KC, Olivier J, Raju S, *Stenting of the venous outflow in chronic venous disease: long-term stent-related outcome, clinical, and hemodynamic result*, J Vasc Surg, 2007, 46(5), 979-90. e1. http://doi.org/10.1016/j.jvs.2007.06.046.
[22] Ng J, Bourantas CV, Torii R, Ang HY, Tenekecioglu E, Serruys PW, et al., *Local hemodynamic forces after stenting: implications on restenosis and thrombosis*, Arterioscler, Thromb, Vasc, 2017, 37(12), 2231-42. http://doi.org/10.1161/ATVBAHA.117.309728.

[23] Oguzkurt L, Tercan F, Ozkan U, Gulcan O, *Iliac vein compression syndrome: outcome of endovascular treatment with long-term follow-up*, Eur J Radiol, 2008, 68(3), 487-92. http://doi.org/10.1016/j.ejrad.2007.08.019.
[24] Poon EK, Barlis P, Moore S, Pan W-H, Liu Y, Ye Y, et al., *Numerical investigations of the haemodynamic changes associated with stent malapposition in an idealised coronary artery*, J Biomech. 2014, 47(12), 2843-51. http://doi.org/10.1016/ijbiomech.2014.07.030.
[25] Poulson W, Kamenskiy A, Seas A, Deegan P, Lomneth C, MacTaggart J, *Limb flexion-induced axial compression and bending in human femoropopliteal artery segments*, J Vasc Surg, 2018, 67(2), 607-13. http://doi.org/ 10.1016/j.jvs.2017.01.071.
[26] Raju S, Tackett Jr P, Neglen P, *Reinterventions for nonocclusive iliofemoral venous stent malfunctions*, J Vasc Surg, 2009, 49(2), 511-8. http://doi.org/10.1016/j.jvs.2008.08.003.
[27] Raju S, Ward Jr M, Kirk O, *A modification of iliac vein stent technique*, Ann Vasc Surg, 2014, 28(6), 1485-92. http://doi.org/10.1016/j.avsg.2014.02.026.
[28] Restaino RM, Holwerda SW, Credeur DP, Fadel PJ, Padilla J, *Impact of prolonged sitting on lower and upper limb micro-and macrovascular dilator function*, Exp Physiol, 2015, 100(10), 829-38. http://doi.org/10.1113/ep085238.
[29] Rollo JC, Farley SM, Jimenez JC, Woo K, Lawrence PF, DeRubertis BG, *Contemporary outcomes of elective iliocaval and infrainguinal venous intervention for post-thrombotic chronic venous occlusive disease*, J Vasc Surg-Venous L, 2017, 5(6), 789-99. http://doi.org/10.1016/j.jvsv.2017.05.020.
[30] Rossi FH, Kambara AM, Rodrigues TO, Rossi CB, Izukawa NM, Pinto IM, et al., *Comparison of computed tomography venography and intravascular ultrasound in screening and classification of iliac vein obstruction in patients with chronic venous disease*, J Vasc Surg-Venous L, 2020, 8(3), 413-22. http://doi.org/10.1016/j.jvs.2023.01.128.
[31] Sakai K, Takahira N, Tsuda K, Akamine AJJoOS, *Effects of intermittent pneumatic compression on femoral vein peak venous velocity during active ankle exercise*, J Orthop Surg-Hong K, 2021, 29(1), 2309499021998105. http://doi.org/10.1177/2309499021998105.
[32] Sakamoto S, Ikado H, Kawarada O, Harada K, Ishihara M, Yasuda S, et al., *Pulsatile high-velocity turbulent flow in lower extremity venous ultrasonography*, Heart, 2014, 100(10), 814-. http://doi.org/ 10.1136/heartjnl-2013-305309.
[33] Saleem T, Raju S, *An overview of in-stent restenosis in iliofemoral venous stents*, , J Vasc Surg-Venous L 2022, 10(2), 492-503. e2. http://doi.org/10.1016/j.jvsv.2021.10.011.
[34] Smouse HB, Nikanorov A, LaFlash D, *Biomechanical forces in the femoropopliteal arterial segment*, Endovascular Today, 2005, 4(6), 60-6. http://doi.org/10.1053/j.tvir.2006.05.003.
[35] Thosar SS, Johnson BD, Johnston JD, Wallace JP, *Sitting and endothelial dysfunction: the role of shear stress*, Med Sci Monitor, 2012, 18, RA173. http://doi.org/10.12659/MSM.883589.
[36] Tresson P, Hublet A, Holdner A, Bordet M, Millon A, Papillard M, et al., *Common Femoral Artery Curvature During Hip Flexion*, CardioVasc Interventional Radiol, 2023, 1-8. http://doi.org/10.1007/s00270-023-03479-x.
[37] Walsh LK, Restaino RM, Martinez-Lemus LA, Padilla J, *Prolonged leg bending impairs endothelial function in the popliteal* artery, Physiol Rep, 2017, 5(20), e13478. http://doi.org/ 10.14814/phy2.13478.
[38] Wang J, Jin X, Huang Y, Ran X, Luo D, Yang D, et al., *Endovascular stent-induced alterations in host artery mechanical environments and their roles in stent restenosis and late thrombosis*, Regener Biomater, 2018, 5(3), 177-87. http://doi.org/org/10.1093/rb/rby006.
[39] Wood NB, Zhao SZ, Zambanini A, Jackson M, Gedroyc W, Thom SA, et al., *Curvature and*

tortuosity of the superficial femoral artery: a possible risk factor for peripheral arterial disease, J Appl Physiol, 2006, 101(5), 1412-8. http://doi.org/10.1152/japplphysiol.00051.2006.

[40] Yang L, Liu J, Cai H, Liu Y, *The clinical outcome of a one-stop procedure for patients with iliac vein compression combined with varicose veins*, J Vasc Surg-Venous L, 2018, 6(6), 696-701. http://doi.org/10.1016/j.jvsv.2018.06.012.

[41] Youn YJ, Lee J, *Chronic venous insufficiency and varicose veins of the lower extremities*, The Korean journal of internal medicine, 2019, 34(2), 269. http://doi.org/10.3904/kjim.2018.230.